Bioorganic & Medicinal Chemistry Letters 20 (2010) 1985–1989

Contents lists available at ScienceDirect

Bioorganic & Medicinal Chemistry Letters

journal homepage: www.elsevier.com/locate/bmcl

Rational design of potent GSK3β inhibitors with selectivity for Cdk1 and Cdk2

Dominique Lesuisse [a,e,*], Gilles Dutruc-Rosset [a,e], Gilles Tiraboschi [c,e], Matthias K. Dreyer [f], Sébastien Maignan [d,e], Alain Chevalier [a,e], Frank Halley [a,e], Philippe Bertrand [b,e], Marie-Claude Burgevin [b,e], Dominique Quarteronet [b,e], Thomas Rooney [b,e]

[a] Medicinal Chemistry, 13 Quai Jules Guesde, 94300 Vitry-sur-Seine, France
[b] CNS Department, 13 Quai Jules Guesde, 94300 Vitry-sur-Seine, France
[c] CAS Molecular Modelling, 13 Quai Jules Guesde, 94300 Vitry-sur-Seine, France
[d] CAS Structural Biology, 13 Quai Jules Guesde, 94300 Vitry-sur-Seine, France
[e] Sanofi-aventis, 13 Quai Jules Guesde, 94300 Vitry-sur-Seine, France
[f] Sanofi-aventis, Industriepark Hoechst, 65926 Frankfurt am Main, Germany

ARTICLE INFO

Article history:
Received 27 November 2009
Revised 18 January 2010
Accepted 20 January 2010
Available online 25 January 2010

Keywords:
Glycogen synthase kinase
GSK3β
Aminoindazole
Cdk's

ABSTRACT

From an HTS hit, a series of potent and selective inhibitors of GSK3β have been designed based on a Cdk2-homology model and with the help of several crystal structures of the compounds within Cdk2.

Glycogen synthase 3β (GSK3β) is one of the two major tau phosphorylating enzymes.[1] As tau hyperphosphorylation has been linked to both cytoskeletal dysfunction and the formation of neurofibrillary tangles, one of the major hallmarks of Alzheimer's disease,[2] inhibiting these events could potentially be beneficial in the treatment of this chronic neurodegenerative disease. In the course of a programme aimed at identifying inhibitors of this enzyme, we initiated a high throughput screening approach. This led to the hit **1** with an IC_{50} in the micromolar range (1.18 μM). The object of the present paper is to describe how we have optimized this hit into potent and selective inhibitors.

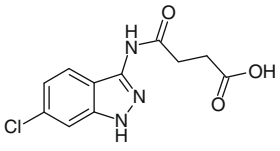

1
IC_{50} = 1.18 μM

At the time this work was initiated, no structural data on GSK3β was available. Based on the 28% identity (45% homology) of GSK3β with Cdk2, we built a homology model from the reported structure of Cdk2.[3] Compound **1** was therefore crystallized with human monomeric Cdk2 (see Supplementary Fig. S1) and the results were transferred into the GSK3β homology model, clearly suggesting that the aminoindazole moiety interacted with the hinge area of the kinase, while the carboxylic acid chain was pointing towards the solvent area (Fig. 1). The model also showed that two important areas of the protein were poorly or not occupied, namely the ribose and the hydrophobic pockets, suggesting that occupying these pockets would have the potential to greatly enhance the affinity of this series for the kinase.

Our medicinal chemistry programme can be summarized as follows: introduce substitutions in the 5- and 6-position of the aminoindazole moiety to improve affinity and replace the carboxylic acid by a chain more amenable to brain penetration (Fig. 2).

As the carboxylic acid chain sits in the solvent area, it was hypothesized that it contributed little to the activity. Indeed removal of the carboxylic acid moiety, as in **2**, resulted in better inhibitor activity (0.35 μM) than the initial hit **1** (1.18 μM). This gain of

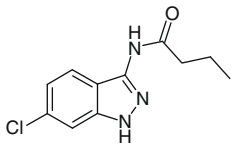

2
IC_{50} = 0.35 μM

* Corresponding author. Tel.: +33 1 58933771; fax: +33 1 58933450.
E-mail address: dominique.lesuisse@sanofi-aventis.com (D. Lesuisse).

0960-894X/$ - see front matter © 2010 Elsevier Ltd. All rights reserved.
doi:10.1016/j.bmcl.2010.01.114

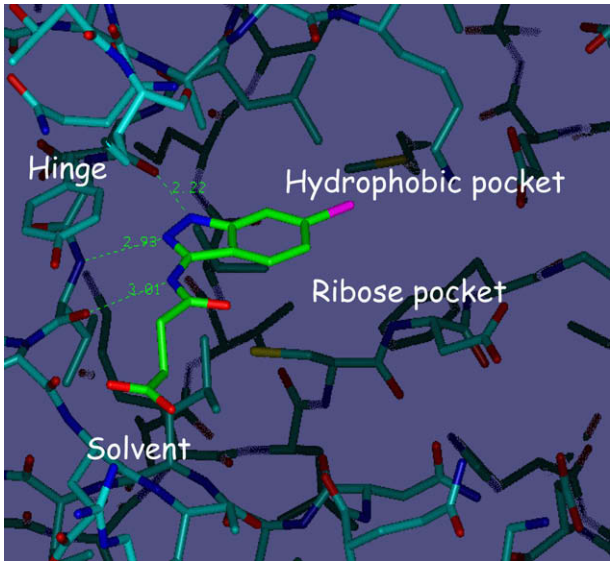

Figure 1. Docking model of **1** into GSK3β.

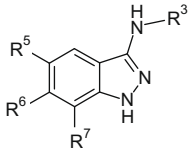

Figure 2.

activity is probably due to less desolvation energy upon binding. We therefore selected **2** as a starting point for further optimization.

We first investigated the hydrophobic pocket. To this end, the chlorine atom in the 6-position was replaced by several groups. While the majority of substitutions were detrimental to the activity, introduction of a phenolic or anilinic group in the 6-position (compounds **3–7**) increased potency by up to 10-fold (Table 1).

We hypothesized that this improvement was linked to a favorable interaction with the catalytic lysine in the bottom of the hydrophobic pocket. Many attempts to obtain a co-crystal structure of **4** with Cdk2 were not successful. However, a co-structure obtained by soaking **4** with the Aurora2 kinase showed that this interaction was not observed (Fig. 3). Nevertheless, since the residues around the DFG motif are displaced by packing interactions, we cannot exclude the possibility that this results from the crystal arrangement. On the other hand, **4** did not show any significant inhibition of Aurora2 (IC_{50} >30 μM) so the better activity on GSK3β could be partly explained by this extra H-bond and stabilization of the ring orientation.

Since, as we had predicted, potentially good inhibitory activity could be gained from the introduction of groups towards the ribose pocket, we decided to keep the chlorine atom of **2** in position 6, while investigating position 5. This turned out to be quite profitable, as some of the disubstituted analogs displayed up to 100-fold improvement in activity, compared to the 6-chloro derivative **2**. A non-substituted phenyl was the best 5-substituent; substitution on the phenyl ring did not improve activity (Table 2). Compound **37** was chosen for further optimization.

A classical approach in medicinal chemistry is to try and combine the best substitutions in the same compound. However, combining the 4-phenol in position 6 with the best substituents of position 5 was detrimental to the activity (Table 3). When aryl groups were introduced at both positions 5 and 6 the level of

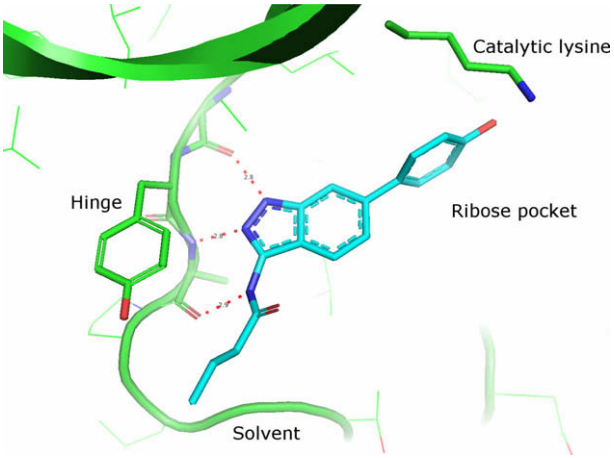

Figure 3. Crystals of Aurora2 kinase domain (125–399CterHistag) with **4** (2.2 Å). Red dashes represent hydrogen bonds to the hinge region of the kinase. The distance between the phenolic OH and the catalytic lysine nitrogen is 4.8 Å.[5]

Table 1
GSK3β activity (IC_{50})[4] of compounds modified in 6-position (Fig. 2)[a]

Compd#	R^6	GSK3β (μM)	Compd#	R^6	GSK3β (μM)
2	Cl	0.354	**20**	$C_6H_5CH_2$–	4.140
3	3,4-$(OH)_2$–C_6H_3–	0.027	**21**	4-F–C_6H_4–	5.008
4	4-OH–C_6H_4–	0.044	**22**	3,5-Cl_2–C_6H_3–	5.413
5	4-OH-2-Cl–C_6H_3–	0.055	**23**	4-F_3CO–C_6H_4–	5.498
6	4-NH_2–C_6H_4–	0.076	**24**	4-MeS–C_6H_4–	7.165
7	3-OH–C_6H_4–	0.094	**25**	$C_6H_5(CH_2)_2$–	8.525
8	CF_3–	0.195	**26**	4-CF_3–C_6H_4–	10.546
9	Br–	0.198	**27**	3-Py	10.892
10	3-Furyl	0.260	**28**	4-Me_2N–C_6H_4–	12.247
11	4-Pyridinyl	0.661	**29**	2-OH-5-Pyridinyl	16.784
12	3-Thienyl	0.935	**30**	4-Me–C_6H_4–	17.103
13	2-NH_2-5-pyridinyl	1.088	**31**	4-CN–C_6H_4–	20.532
14	4-OBn–C_6H_4–	1.184	**32**	3,4-Dioxolano-C_6H_4–	25.038
15	C_6H_5–	1.281	**33**	4-NO_2–C_6H_4–	>100
16	2-Cl–C_6H_4–	1.353	**34**	4-MeO–C_6H_4–	>100
17	(*E*)-CH_3CH=CH–	2.459	**35**	4-Et–C_6H_4–	>100
18	3,5-F_2–C_6H_3–	2.894	**36**	4-Cl–C_6H_4–	>100
19	4-*t*Bu–C_6H_4–	3.808			

[a] R^3 = C(O)*n*-Pr, R^5 = H.

Table 2
GSK3β activity (IC_{50}) of compounds modified in 5-position Fig. 2)[a]

Compd#	R^5	GSK3β (nM)	Compd#	R^5	GSK3β (nM)
2	H	354	**42**	4-Me–C_6H_4–	**14**
37	C_6H_5–	7	**43**	4-NO_2–C_6H_4–	**18**
38	4-NH_2–C_6H_4–	8	**44**	4-F–C_6H_4–	**22**
39	4-OH–C_6H_4–	10	**45**	4-BnO–C_6H_4–	**23**
40	3-Furyl–	11	**46**	4-Pyridinyl	**50**
41	4-Et–C_6H_4–	12	**47**	Br–	**55**

[a] R^3 = C(O)*n*-Pr, R^6 = Cl.

Table 3
GSK3β activity of compounds combining the best substitutions at 5 and 6-positions (Fig. 2)[a]

Compd#	R^5	R^6	GSK3β (nM)
48	2-Furyl–	4-OH–C_6H_4–	14
49	3-Pyridinyl–	4-OH–C_6H_4–	149
50	4-Et–C_6H_4–	4-OH–C_6H_4–	49
51	3-Furyl–	4-OH–C_6H_4–	98
52	4-OH–C_6H_4–	4-OH–C_6H_4–	56
53	4-OBn–C_6H_4–	4-OBn–C_6H_4–	>10,000
54	C_6H_5–	4-OH–C_6H_4–	55
55	C_6H_5–	C_6H_5–	1720
56	Br–	4-OH–C_6H_4–	5

[a] R^3 = C(O)*n*-Pr.

inhibitory activity decreased to that of one of the monosubstituted aryl derivatives in Table 1. The only combinations that proved successful were aryl and halogen at position 5 or 6, such as in **59** or compounds **37–41** from Table 2.

The superposition of the crystal structures of compounds **37** and **57** in Cdk2 shows that the bulky aromatic substituent introduces some small, but significant, changes (Fig. 4) that might account for the lower affinity of **57**. The plane of the indazole ring,

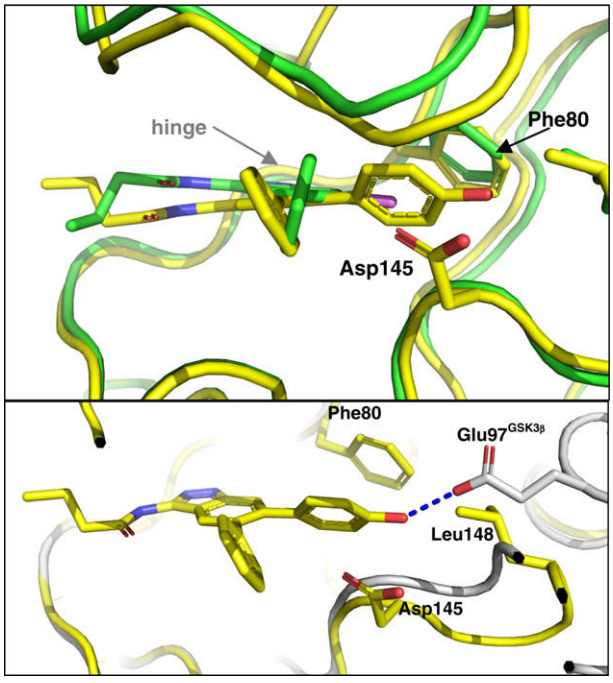

Figure 4. (Top), Superposition of **57** (yellow) and **37** (green) in Cdk2. The hinge segment is behind the inhibitors. For clarity, side chains are only shown for the gate keeper residue Phe80 and for Asp145. (Bottom), Superposition of the Cdk2:**57** complex (yellow) with GSK3β (grey, protein chain taken from PDB 1Q4L), showing the potential interaction of the phenolic hydroxy group with Glu97GSK3β (blue dashes).[5,6]

Table 4
Selectivity of **37** versus a panel of kinases

Kinase	% Inhibition of 37 at 20 μM	Kinase	% Inhibition of 37 at 20 μM
EGF-tyrosine kinase (h)	−24	MAP kinase (ERK 42)	13
CAM kinase II	−10	MEK1 kinase	13
Plk1	−6	Protein kinase C-a (h)	14
Akt	−2	Protein kinase A (stimulated)	21
Protein kinase p56lck	−2	Aurora	34
Src kinase (h)	−2	Casein kinase II (h)	38
Fak	1	ZAP70 kinase (h)	45
Pak3	2	Jnk3	58
Abl	3	cdk4	72
IGF1R	5	cdk1	95
p38	5	Cdk2	93
Tie2	7		

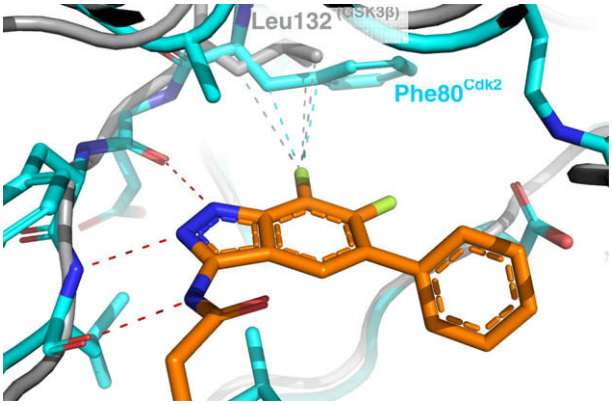

Figure 5. Superimposition of the crystal structure of **60** (orange) in Cdk2 (cyan) with GSK3β (grey; protein chain taken from PDB 1Q4L). Nonpolar interactions between the 7-fluorine and Cdk2 gate keeper Phe80 are indicated by cyan dashes. Corresponding distances to GSK3β residue Leu132 are shown in grey. Hydrogen bonds to the backbone atoms of the hinge segment are depicted with red dashes.

including the butyramide, is inclined by about 12° with respect to the inhibitor position of **37**. In addition, the conformation of the phenyl ring in the 5-position of **57** is rotated by 40° with respect to **37** due to intramolecular repulsion between R5 and R6. The orientation of the 6-phenol on this part is determined by the protein environment, in particular the main chain at Asp145 and the gate keeper residue Phe80.

In related crystal structures with smaller substituents (not shown) both the orientation of the aromatic plane along the hinge, as well as the orientation of an aryl moiety in the 5-position, resemble those seen in **37** and suggest that this is a preferred conformation within the binding pocket.

Table 5
Effect of a halogen in position 7 on the selectivity of 5,6-substituted 3-aminoindazoles[a]

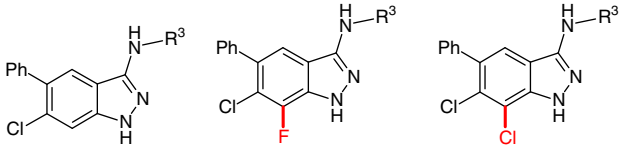

Compd#	**37**	**57**	**58**
GSK3β (nM)	7	6	12
Cdk1 (nM)	100	2500	—
Cdk2 (nM)	2500	3160	>10,000

[a] R^3 = C(O)*n*-Pr.

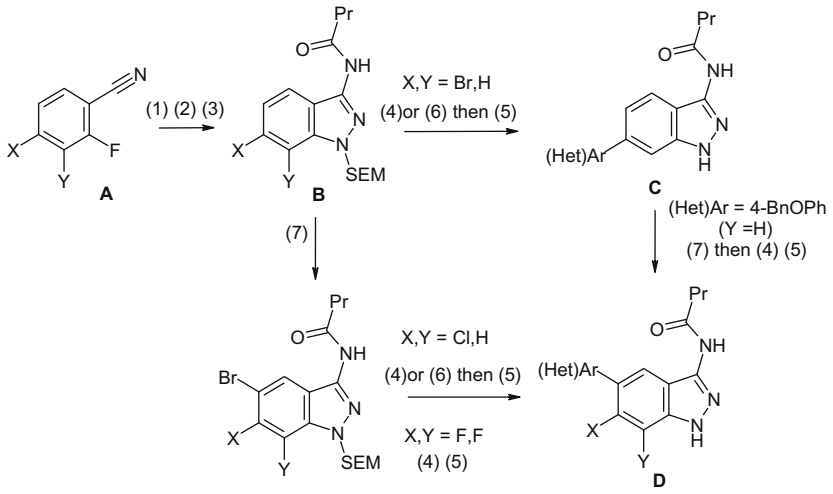

Scheme 1. Reagents and conditions: (1) $NH_2NH_2{\cdot}H_2O$; EtOH; X, Y = Br, H (90%), Cl, H (93%), F, Cl (26%), F, F (42%); (2) *n*PrCOCl/Py (80%-Q); (3) SEMCl/NaH/DMF/RT (31–61%); (4) (Het)ArB$(OH)_2$/Pd[$P(Ph_3)]_4$/Na_2CO_3/dioxane/H_2O; (5) Bu_4NF/THF/reflux; (6) $Pd(dba)_2$/PPh_3/bis(pinacolato)diborane/AcOK/dioxane/H_2O; (Het)ArBr/Pd[$P(Ph)_3]_4$/Na_2CO_3/dioxane/H_2O; (7) Br_2/$CHCl_3$/Py X,Y = Cl,H (75%), F,F (36%).

Once again, no hydrogen bond between the hydroxyl from the phenol and the protein could be observed, but this is likely to be different in GSK3β where the conserved $Glu97^{GSK3\beta}$ carboxylate is near the position of $Leu148^{CDK2}$ of our surrogate and may form a hydrogen bond with the inhibitor OH group.

With this SAR, and taking into account the generally poor PK properties of phenols resulting from phase II metabolism and elimination and the propensity of anilines to give Ames positive results, we chose to keep **37** for further optimization. An important aspect of this programme is the selectivity of the compounds for other kinases. Pan kinase inhibitors, even if tolerated in cancer treatment, are probably not suitable for the prolonged treatment of chronic diseases, such as Alzheimer's disease. **37** displayed good selectivity versus a panel of kinases[7] belonging to the 4 major kinase classes, AGC, CMGC, CLK and TK[8] (Table 4).

However, **37** displayed potent inhibition of Cdk1 and Cdk2 (0.1 and 2.5 μM, respectively). As Cdk's and GSK3β belong to the same family of CMGC kinases, they share a high degree of sequence and structural homology. Indeed, several reported inhibitors of GSK3β are non-selective vs. Cdks.[9,10] Particularly noteworthy in this respect are the reported series of pyrazolo[3,4-*b*]pyridine and pyrazolo[3,4-*b*]pyridazine GSK3β inhibitors, [11] as these compounds are quite similar to the ones described in this Letter in terms of structures and binding modes. These authors were able to successfully address the Cdk2 selectivity of their series by introducing a basic function in a position equivalent to our position 3 which resulted in a steric/electronic clash with a salt bridge present in Cdk2 but not in GSK3b.[12] This concept was also applied successfully in the case of a series of 4-acylamino-6-arylfuro[2,3-*d*]pyrimidines.[13] In our case, a close comparison of the ATP-binding site of both kinases revealed a significant difference regarding the nature of their gate keeper residues. This residue controls access to a hydrophobic pocket not exploited by ATP.[14] This structural difference has been previously used to tune the selectivity for protein kinases.[15] While GSK3β has a leucine, Cdks have a phenylalanine at this position. This amino acid is bulkier (see Fig. 5) and when looking at the model of our aminoindazoles in the protein, it clearly appeared that the interaction of position 7 was pointing right towards the gate keeper residue and that introduction of a small substituent in this position, while acceptable for GSK3β, could de detrimental to Cdks' activity.

This turned out to be the case, as shown in Table 5. When a fluorine was introduced in the 7-position (**60**), activity on GSK3β was maintained but activity on Cdk1 was lowered by 20-fold. The superposition of the crystal structure of **60** complexed to Cdk2 and the crystal structure of GSK3β,[16] which became available in the later stage of our project, nicely shows the unfavourably close contact of the 7-fluorine to the gate keeper Cdk2-Phe80, while the corresponding Leu132 in GSK3β leaves significantly more space (Fig. 5). Introduction of the larger chlorine was even able to totally abolish the Cdk2 activity (**58**), but only marginally affected the activity on GSK3β.

The synthesis of these compounds was straightforward and largely derivative, as illustrated in Scheme 1.[17] The aminoindazole moiety **B** was built from a halo substituted aryl cyanide **A** by reaction with hydrazine, followed by propyl amide introduction and SEM protection. The halogen atom in **B** was replaced by an aryl or heteroaryl group upon either direct Suzuki coupling with an arylboronic acid, or via an intermediate pinacolborane to afford monosubstituted aminoindazoles **C** (from Table 1). A 5-bromine could be introduced by bromination of **B** and **C**, that could be further substituted by an aryl or heteroaryl group using the same strategy, leading to aminoindazoles **D** bearing one or two aryl or heteroaryl groups in the 5- and 6-positions (compounds from Tables 2 and 3).

From a homology model built from Cdk2 and several co-crystal structures of inhibitors with Cdk2, a series of potent GSK3β inhibitors were designed. The model was also used to understand and build in selectivity versus Cdk's for these compounds. These compounds displayed good cellular inhibition of Tau phosphorylation.[18] However, their poor ADME properties made it difficult to obtain reliable in vivo activities. Optimization of these parameters will be the object of a following paper.

Acknowledgements

We are grateful to the analytical department for compound analyses.

Supplementary data

Supplementary data associated with this article can be found, in the online version, at doi:10.1016/j.bmcl.2010.01.114.

References and notes

1. Flaherty, D. B.; Soria, J. P.; Tomasiewicz, H. G.; Wood, J. G. *J. Neurosci. Res.* **2000**, *62*, 463; Brunden, K. R.; Trojanowski, J. Q.; Lee, V. M.-Y. *Nat. Rev. Drug Disc.* **2009**, *8*, 783.

2. Maccioni, R. B.; Munoz, J. P.; Barbeito, L. *Arch. Med. Res.* **2001**, *32*, 367.
3. De Bondt, H. L.; Rosenblatt, J.; Jancarik, J.; Jones, H. D.; Morgan, D. O.; Kim, S. H. *Nature* **1993**, *363*, 595.
4. Technical note: measurement of GSK3β enzymatic activity by Scintillation Proximity Assay (SPA). Partially purified recombinant human GSK3β enzyme is incubated for 30 min at 20 °C in 96-W microplates with 1 μM ATP (including 50 nCi γ-^{33}P]-33P]-ATP/well) and 0.8 μM of pGS-2 peptide substrate (Upstate Biotechnology Inc.) in the presence of tested compound, and in HEPES buffer (40 mM, pH 7.4, supplemented with 200 μM EDTA, 10 mM MgCl2, 1 mM DTT and 0.1 mg/ml BSA). Enzymatic reaction is stopped by adding SPA-streptavidine beads (GE Healthcare) concentrated (6 mg/ml) in PBS (containing 20 mM ATP, 25 mM EDTA and 0.2% triton X-100) under 10 min. agitation. Radioactivity is measured by using a scintillation liquid reader (1450 Microbeta™, Perkin–Elmer). IC_{50} values are calculated by non-linear regression analysis with Excel/XL fit software (IDBS).
5. Figures were produced using PyMOL: DeLano, W.L. The PyMOL Molecular Graphics System (2002) on World Wide Web http://www.pymol.org, Crystal structure of **4** with Aurora has been deposited in the PDB with accession codes 3LAU.
6. Crystal structures of **37**, **57** and **60** with Cdk2 have been deposited in the PDB with accession codes 3LFS, 3FLN, and 3LFQ.
7. Internal profiling.
8. Niwa, T. *J. Chem. Inf. Model.* **2006**, *46*, 2158.
9. See for instance: Mettey, Y.; Gompel, M.; Thomas, V.; Garnier, M.; Leost, M.; Ceballos-Picot, I.; Noble, M.; Endicott, J.; Vierfond, J.-M.; Meijer, L. *J. Med. Chem.* **2003**, *46*, 222.
10. Bain, J.; McLauchlan, H.; Elliott, M.; Cohen, P. *Biochem. J.* **2003**, *371*, 199.
11. Witherington, J.; Bordas, V.; Garland, S. L.; Hickey, D. M. B.; Ife, R. J.; Liddle, J.; Saunders, M.; Smith, D. G.; Ward, R. W. *Bioorg. Med. Chem. Lett.*, 2003. 1577.
12. Witherington, J.; Bordas, V.; Haigh, D.; Hickey, D. M. B.; Ife, R. J.; Rawlings, D. A.; Slingsby, B. P.; Smith, D. G.; Ward, R. W. *Bioorg. Med. Chem. Lett.* **2003**, *13*, 1581.
13. Yutaka Maeda, Y.; Nakano, M.; Sato, H.; Miyazaki, Y.; Schweiker, S. L.; Smith, J. L.; Truesdale, A. T. *Bioorg. Med. Chem. Lett.* **2004**, *14*, 3907.
14. Klebl, B. M.; Müller, G. *Exp. Opin. Ther. Targets* **2005**, *9*, 975.
15. Shimamuraa, T.; Shibataa, J.; Kuriharaa, H.; Mitaa, T.; Otsukia, S.; Sagaraa, T.; Hiraia, H.; Iwasawa, Y. *Bioorg. Med. Chem. Lett.* **2006**, *16*, 3751. and references cited therein; Gambacorti-Passerini, C. *J. Med. Chem.* **2006**, *49*, 5759; Shokat, K. M. *Nat. Chem. Biol.* **2007**, 229.
16. Bertrand, J. A.; Thieffine, S.; Vulpetti, A.; Cristiani, C.; Valsasina, B.; Knapp, S.; Kalisz, H. M.; Flocco, M. *J. Mol. Biol.* **2003**, *333*, 393.
17. Dutruc, Rosset, G.; Lesuisse, D.; Rooney, T.; Halley, F. Fr. Demande FR 2836915 A1, 2003; *Chem. Abstr.* **2003**, *139*, 246027; Lesuisse, D.; Dutruc-Rosset, G.; Halley, F.; Babin, D.; Rooney, T.; Tiraboschi, G. PCT Int. Appl. WO 2004062662 A1, 2004; *Chem. Abstr.* **2004**, *141*, 140438.
18. Briefly, brain slices (300 μm) are prepared from cerebral cortex of 10 week-old rats, and slice suspension (50 μl/microtube) is incubated in DMEM (containing pyruvate and 4.5 g/l glucose) with tested compound in a final volume of 500 μl, for 120 min at 37 °C under mild agitation. Incubation is stopped by centrifugation, followed by lysis and sonication at 4 °C. Lysates are then centrifuged (18,000*g*, 15 min, 4 °C), and the supernatants are used for protein dosage, and subsequent western blotting analysis. SDS–PAGE electrophoresis is performed in MOPS-SDS denaturating conditions; the phosphorylation of tau protein is detected by using AD2 mouse monoclonal antibody specific for Ser396/404 phosphoepitope as primary antibody, and peroxydase-labelled mouse antiserum as secondary antibody for measuring signal by chemiluminescence. Analysis of autoradiogrammes by 'GeneTools' software (Syngene, GeneGnome, Ozyme) was performed for IC_{50} estimation. In these conditions, **37** and **57** displayed IC_{50}'s of inhibition of 400 and 250 nM, respectively.